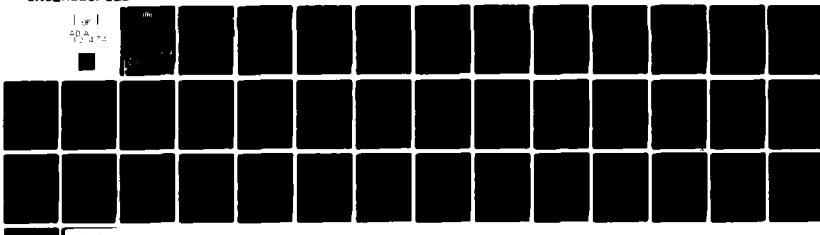


AD-A101 474      NAVAL UNDERWATER SYSTEMS CENTER NEW LONDON CT NEW LO-ETC F/6 12/1  
AN AID IN STEEPEST DESCENT EVALUATION OF INTEGRALS. (U)  
FEB 81   A H NUTTALL

UNCLASSIFIED   NUSC-TR-6433

NL

1 of 1  
40A272



END  
DATE  
FILED  
8-81  
DTIC

50

NUSC Technical Report 8433  
27 February 1981

12

# LEVEL II

## An Aid in Steepest Descent Evaluation of Integrals

Albert H. Nuttall  
Surface Ship Sonar Department

AD A 101474



**Naval Underwater Systems Center**  
Newport, Rhode Island / New London, Connecticut

50  
DMC FILE COPY

Approved for public release; distribution unlimited.

50  
S DTIC  
ELECTED  
JUL 1 7 1981  
D  
F

81 7 16 102

## Preface

This research was conducted under NUSC IR/IED Project No. A75205, Sub-project No. ZR0000101, *Applications of Statistical Communication Theory to Acoustic Signal Processing*, Principal Investigator, Dr. A. H. Nuttall (Code 3302), Program Manager, Capt. David F. Parrish, Naval Material Command (MAT 08L).

The Technical Reviewer for this report was P. B. Abraham (Code 3331).

**Reviewed and Approved: 27 February 1981**

*William A. Von Winkle*  
W. A. Von Winkle  
Associate Technical Director  
for Technology

The author of this report is located at the  
New London Laboratory, Naval Underwater Systems Center  
New London, Connecticut 06320.

DD FORM 1 JAN 73 1473 EDITION OF 1 NOV 68 IS OBSOLETE  
S/N 0102-014-6601

40392 8  
11/1

## Table of Contents

	Page
List of Illustrations . . . . .	i
List of Symbols . . . . .	iii
Introduction . . . . .	1
Explanation of Technique . . . . .	2
Examples . . . . .	4
Summary . . . . .	25
Appendix A — Computer Programs . . . . .	A-1
Appendix B — Steepest Descent for General Analytic Function . . . . .	B-1
References . . . . .	R-1

## List of Illustrations

Figure	Page
1 Steepest Descent Directions for Airy Function, $\theta=0$ .....	5
2 Steepest Descent Directions for Airy Function, $\theta=3\pi/4$ .....	6
3 Steepest Descent Directions for Airy Function, $\theta=\pi$ .....	7
4 Steepest Descent Directions for Hankel Function, $\beta=0.5$ .....	9
5 Steepest Descent Directions for Hankel Function, $\beta=1$ .....	10
6 Steepest Descent Directions for Hankel Function, $\beta=1.5$ .....	11
7 Steepest Descent Directions for Klein-Gordon Equation, $\theta=0.8$ ..	13
8 Steepest Descent Directions for $\exp(w(z))=z \exp\left(\frac{-K}{z-1}\right)$ , $K=3$ ..	14
9 Steepest Descent Directions for Cubic, $\alpha=0$ .....	15
10 Steepest Descent Directions for Cubic, $\alpha=5\pi/12$ .....	16
11 Steepest Descent Directions for Cubic, $\alpha=3\pi/4$ .....	17
12 Zero Locations for $A=0.35$ .....	20
13 Steepest Descent Contour for $A=0.35$ , $t=2$ .....	21
14 Descent Contours for $A=0.35$ , $t=5$ .....	23

**List of Symbols**

$z$	complex variable
$C$	contour in $z$ -plane
$g(z)$	amplitude function in integral
$w(z)$	exponent function in integral
$\lambda$	large parameter
$z_s$	saddle point location
$x, y$	real and imaginary parts of $z$
$u, v$	real and imaginary parts of $w$
$\nabla$	gradient operator
$(\ )_b^{1/2}$	particular branch of square root
$(\ )^{1/2}$	principal square root
$z_0$	zero location

## Introduction

The evaluation of contour integrals with analytic integrands is often accomplished by moving the contour to an equivalent one, such that the integrand is better behaved or can be approximated more easily. In particular, movement of the original contour to one that takes advantage of saddle points of the integrand or paths of descent or steepest descent is a very fruitful procedure. It is presumed that the reader is familiar with this technique; see references 1-3, for example. However, one of the difficulties of this procedure is determining the locations of the steepest descent contours (reference 1, p. 263). For complicated integrands, especially those involving branches of multivalued functions, exact determination of steepest descent contours is virtually impossible analytically, and recourse to some type of computer aid is recommended. The procedure given here does not require solution of nonlinear equations, but does give a very good indication of steepest descents with a minimum of analytical and programming effort.

### Explanation of Technique

Suppose we wish to evaluate the contour integral

$$\int_C dz \ g(z) \ \exp(\lambda w(z)) \ , \quad (1)$$

where  $g(z)$  and  $w(z)$  are analytic functions of  $z$ , except for isolated singularities such as poles, essential singularities, and branch points; and  $C$  is a contour (finite or infinite) in the complex  $z$ -plane. The saddle points of the exponential in (1) occur where (reference 1, p. 258)

$$w'(z_s) = 0 \ . \quad (2)$$

For  $\lambda$  real, the standard method of determining the paths of steepest descent out of a saddle point is to keep the imaginary part of  $w(z)$  constant and equal to its value at  $z_s$  (reference 1, p. 255). This generally leads to difficult transcendental equations that must be analytically investigated approximately or solved numerically.

An alternative procedure for finding the steepest descent directions at any point in the  $z$ -plane is as follows: Let

$$\begin{aligned} z &= x + iy \ , \\ w(x + iy) &= u + iv \ . \end{aligned} \quad (3)$$

Then the magnitude of the exponential in (1) is  $\exp(\lambda u)$ , and its direction of steepest descent at  $x, y$  is proportional to the negative of the gradient (reference 1, p. 254):

$$\nabla \exp(\lambda u) = \lambda \exp(\lambda u) \ \nabla u \ , \quad (4)$$

where

$$\nabla u = \frac{\partial u}{\partial x} \vec{a}_x + \frac{\partial u}{\partial y} \vec{a}_y \ , \quad (5)$$

and  $\vec{a}_x$  and  $\vec{a}_y$  are unit vectors in the positive  $x$ - and  $y$ -directions, respectively. The explicit evaluation of (5) requires that one analytically evaluate  $u = \operatorname{Re}\{w(x + iy)\}$  and then analytically derive  $\partial u / \partial x$  and  $\partial u / \partial y$ . This can be tedious and is liable to human error.

An alternative simpler procedure is possible: By the Cauchy-Riemann conditions applied to a function analytic at  $z$ , the derivative

$$\begin{aligned} w'(z) &= \frac{\partial u}{\partial x} + i \frac{\partial v}{\partial x} \\ &= \frac{\partial v}{\partial y} - i \frac{\partial u}{\partial y} \ . \end{aligned} \quad (6)$$

That is, we can express the desired partial derivatives as

$$\frac{\partial u}{\partial x} = \operatorname{Re}\{w'(z)\}, \quad \frac{\partial u}{\partial y} = -\operatorname{Im}\{w'(z)\} \ . \quad (7)$$

Then the negative of the gradient in (5) can be written as

$$-\nabla u = -\operatorname{Re}\{w'(z)\} \vec{a}_x + \operatorname{Im}\{w'(z)\} \vec{a}_y . \quad (8)$$

So if we evaluate  $w'(z)$ , the direction of steepest descent at any point  $z$  has components in the  $x, y$  directions proportional to

$$-\operatorname{Re}\{w'(z)\}, \operatorname{Im}\{w'(z)\} \quad (9)$$

for  $w'(z) \neq 0$ . The only analytical calculation necessary is that of derivative  $w'(z)$ , a task generally easily accomplished, and indeed necessary for evaluation of saddle point locations anyway. A computer program can then be written to numerically evaluate  $w'(z)$  in terms of its components (9) at all points of interest in the  $z$ -plane. A program for this procedure is given in appendix A, along with the specific examples displayed later in this report.

Presentation of this steepest descent information for human interpretation is accomplished here by drawing a short standard-size line through each point  $z = x + iy$ , centered on the point and with an arrowhead pointing in the direction of steepest descent. The magnitude of the rate of steepest descent is discarded; only the direction is preserved. How effective this procedure is will be demonstrated by the following examples.

## Examples

### Airy Function

The Airy function,  $Ai$ , is proportional to (1) when  $g(z) = 1$ ,

$$w(z) = z - \frac{1}{3}z^3, \quad (10)$$

and  $C$  is an infinite contour starting anywhere in the angular range  $-5\pi/6 < \arg(z) < -\pi/2$  and ending in  $\pi/2 < \arg(z) < 5\pi/6$ ; see reference 1, pp. 52 and 266. Then

$$w'(z) = 1 - z^2. \quad (11)$$

A computer need only evaluate the complex product  $z \cdot z$  and subtract it from 1 in order for (11) to be used in (9). An example of this procedure is given in figure 1. The arrows clearly indicate the steepest descent paths from any point in the  $z$ -plane. The two solutions of (11) equal to zero, namely, saddle points  $z_s = \pm 1$ , have arrows pointing both inward and outward at these points, reflecting the very nature of a saddle point. Movement of the original contour  $C$  to the steepest descent contours (solid lines) out of the saddle point at  $z_s = -1$  is easily accomplished; no singularities of the integrand of (1) are crossed in the movement process.

The Airy function for complex argument (reference 1, section 7.3) has, more generally,

$$w(z) = z \exp(i\theta) - \frac{1}{3}z^3. \quad (12)$$

Figure 1 corresponded to  $\theta = 0$ . For  $\theta \neq 0$ , the determination of steepest descent paths is analytically difficult (ibid.). However, since

$$w'(z) = \exp(i\theta) - z^2, \quad (13)$$

computer evaluation of (13) and (9) is trivial. The steepest descent directions for  $\theta = 3\pi/4$ , for example, are depicted in figure 2. The solid lines in the neighborhood of the saddle points were hand-drawn upon observation of the descent arrows. The interpretation of figure 2 is much easier than its counterpart in reference 1, figure 7.3.3. Also the determination of an equivalent contour to  $C$  is easily achieved by reference to figure 2. First let the new contour come from  $\infty \exp(-i2\pi/3)$  along a steepest ascent to the saddle point at  $z_s = \exp(-i5\pi/8)$ . Then let it continue in a northeasterly direction along the steepest descent direction out of this saddle point to the  $y$ -axis. Next proceed due north to a point near  $z = i$  and then follow a steepest descent path out to  $\infty \exp(i2\pi/3)$ . The vertical portion of this new contour is not a path of steepest descent, but it is obviously a path of descent because the projections of the arrows on this vertical section all point in the upward direction of travel. This discussion also points out that the other saddle point at  $z_s = \exp(i3\pi/8)$  does not enter into the asymptotic development of  $Ai$ , at least for this value of  $\theta$ .

An alternative equivalent contour to  $C$  is the pair of steepest descent contours passing through the saddle points and connecting  $\infty \exp(-i2\pi/3)$  to  $+\infty$  and  $+\infty$  to  $\infty \exp(i2\pi/3)$ , respectively; see figure 2. Observe that the movement of  $C$  to this new

pair of paths is not an approximation; it is an alternative exact representation of the original integral. If one now approximates these two path integrals by their contributions near their peaks at the saddle points, the saddle point at  $z_s = \exp(i3\pi/8)$  will yield exponentially small contributions relative to that at  $z_s = \exp(-i5\pi/8)$ . This can be seen from figure 2 by drawing a straight line between the two saddle points; all projections of arrows along this line point at the upper-right saddle point, meaning that the value of  $|\exp(\lambda w(z))|$  is smaller there.

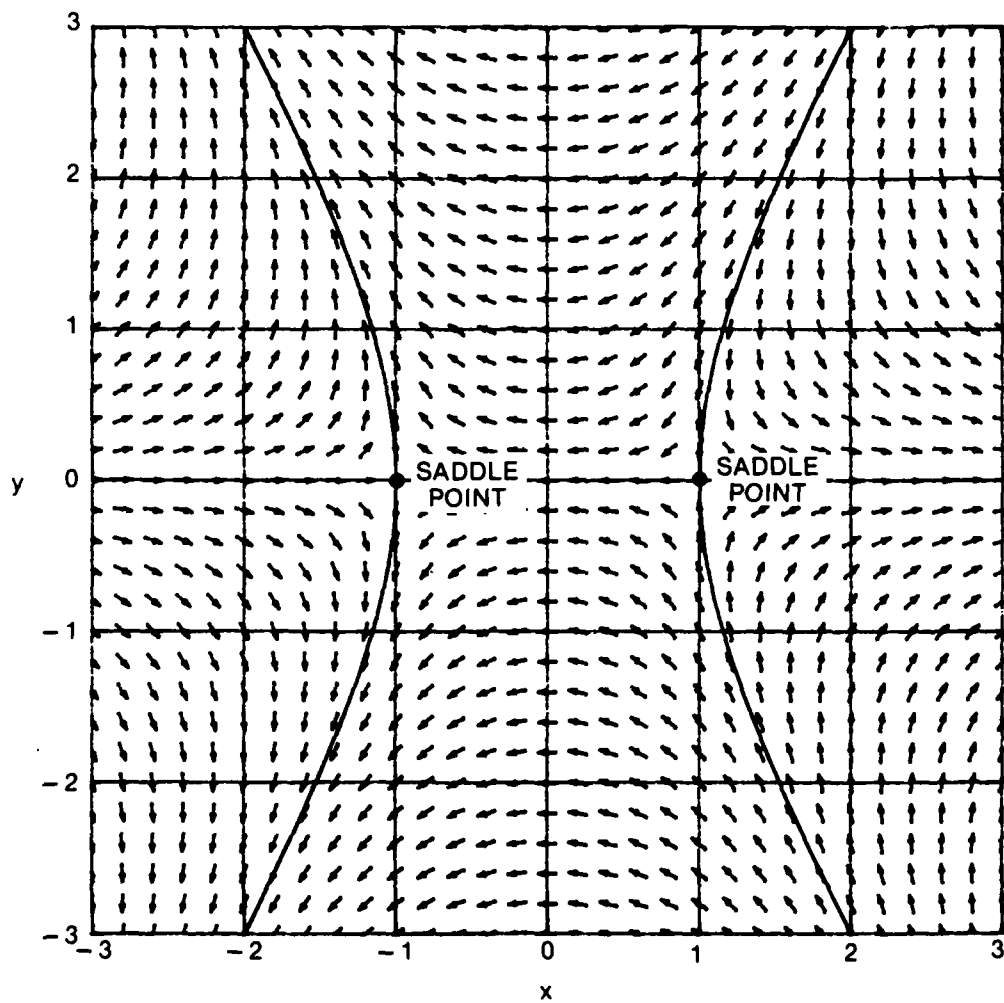


Figure 1. Steepest Descent Directions for Airy Function,  $\theta = 0$

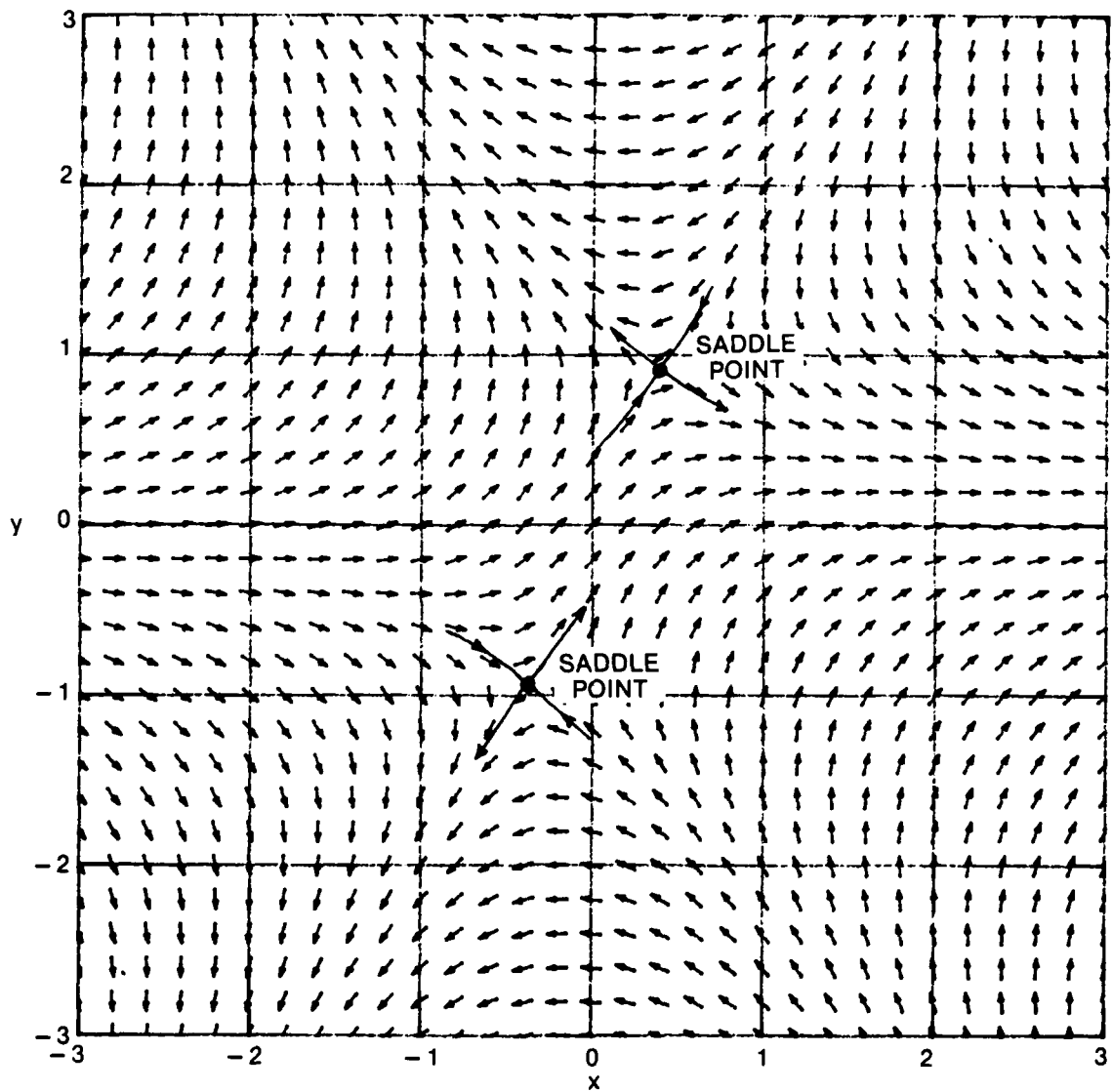


Figure 2. Steepest Descent Directions for Airy Function,  $\theta = 3\pi/4$

When we continue on to the case  $\theta = \pi$  in (12), the character of steepest descents is as depicted in figure 3. Now the straight line connecting the two saddle points has all arrows perpendicular to it; thus this vertical line is a contour of constant  $|\exp(\lambda w(z))|$ . This means that both saddle points contribute equally to the value of integral (1). Again the pair of steepest descent contours through the saddle points (mentioned in the above paragraph) represent exactly the original integral; one could evaluate the original integral exactly by adding the total contributions of both of these paths, or an approximation can be achieved by computing the integrand near its peaks at the saddle points.

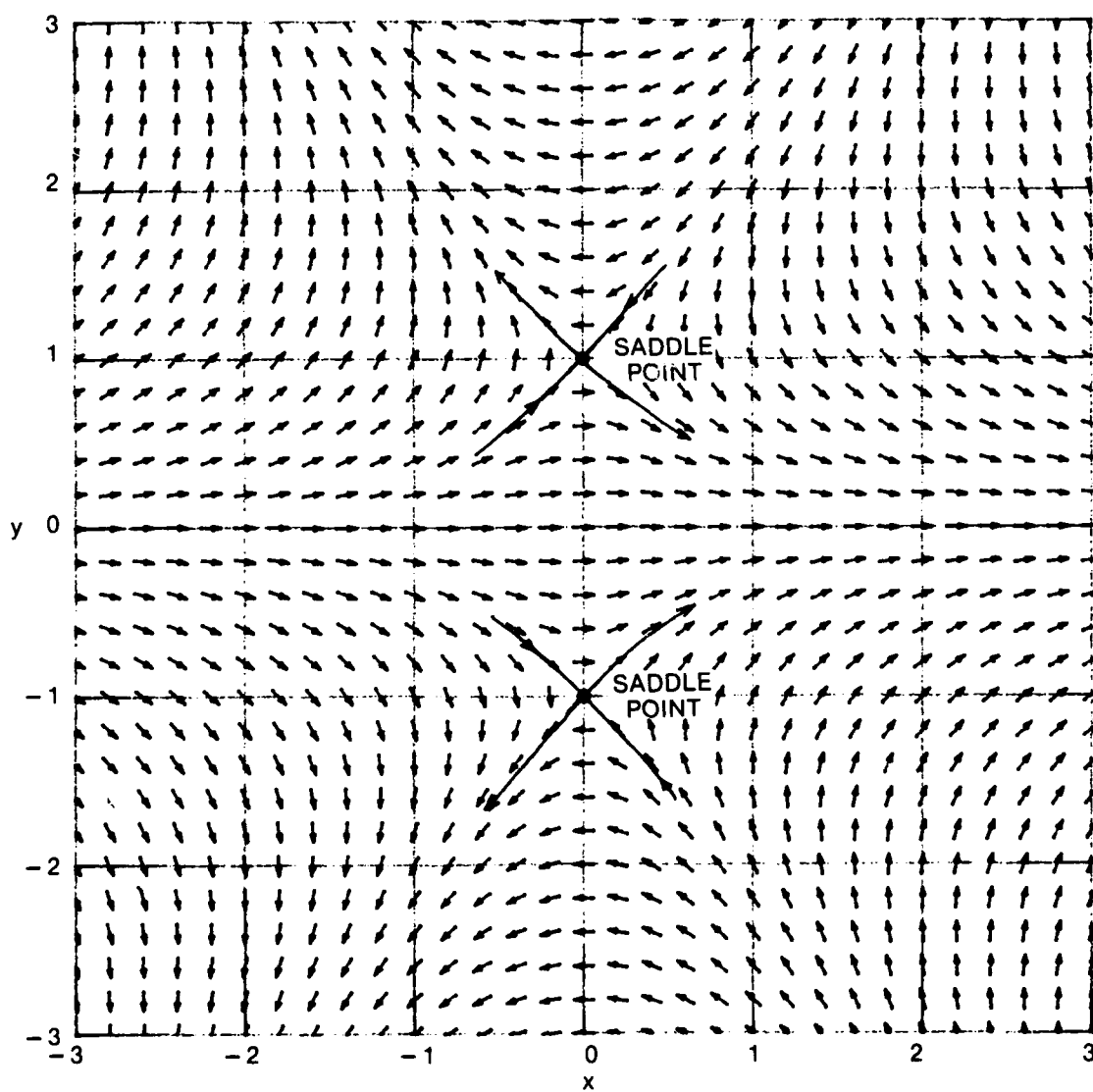


Figure 3. Steepest Descent Directions for Airy Function,  $\theta = \pi$

### Hankel Function

The Hankel function takes the form (reference 1, 7.2.23)

$$w(z) = i[\cos(z) + \beta(z - \frac{i}{2})], \quad (14)$$

where  $\beta$  is a constant. There follows immediately

$$w'(z) = i[-\sin(z) + \beta]. \quad (15)$$

Computer evaluation of (15) requires only a trigonometric sin of a complex number, followed by subtraction and multiplication. Sample descent direction plots for  $\beta = 0.5, 1$ , and  $1.5$  are given in figures 4-6, respectively. (It is informative to compare these figures with figures 7.2.1-7.2.4 in reference 1.) Movement to equivalent contours is obvious from figures 4-6. Since (15) has period  $2\pi$  in  $x$ , only a  $2\pi$  strip has been plotted in figures 4-6. The character of the steepest descents in figure 5 for  $\beta = 1$  is different, in that the saddle points have coalesced; however, there is no difficulty ascertaining from the plots what new contour to adopt.

### Klein-Gordon Equation

This example is complicated by the presence of branch lines in the exponent function  $w(z)$ . Specifically we have (reference 1, 7.5.9)

$$w(z) = i\left[\theta(z^2 - 1)\frac{1}{b}^{1/2} - z\right], \quad (16)$$

where the branch of the square root is taken as positive real for  $z = x > 1$ , and with branch lines extending vertically downward from the branch points at  $z = \pm 1$ . The derivative of (16) is

$$w'(z) = i\left[\frac{\theta z}{(z^2 - 1)\frac{1}{b}^{1/2}} - 1\right], \quad (17)$$

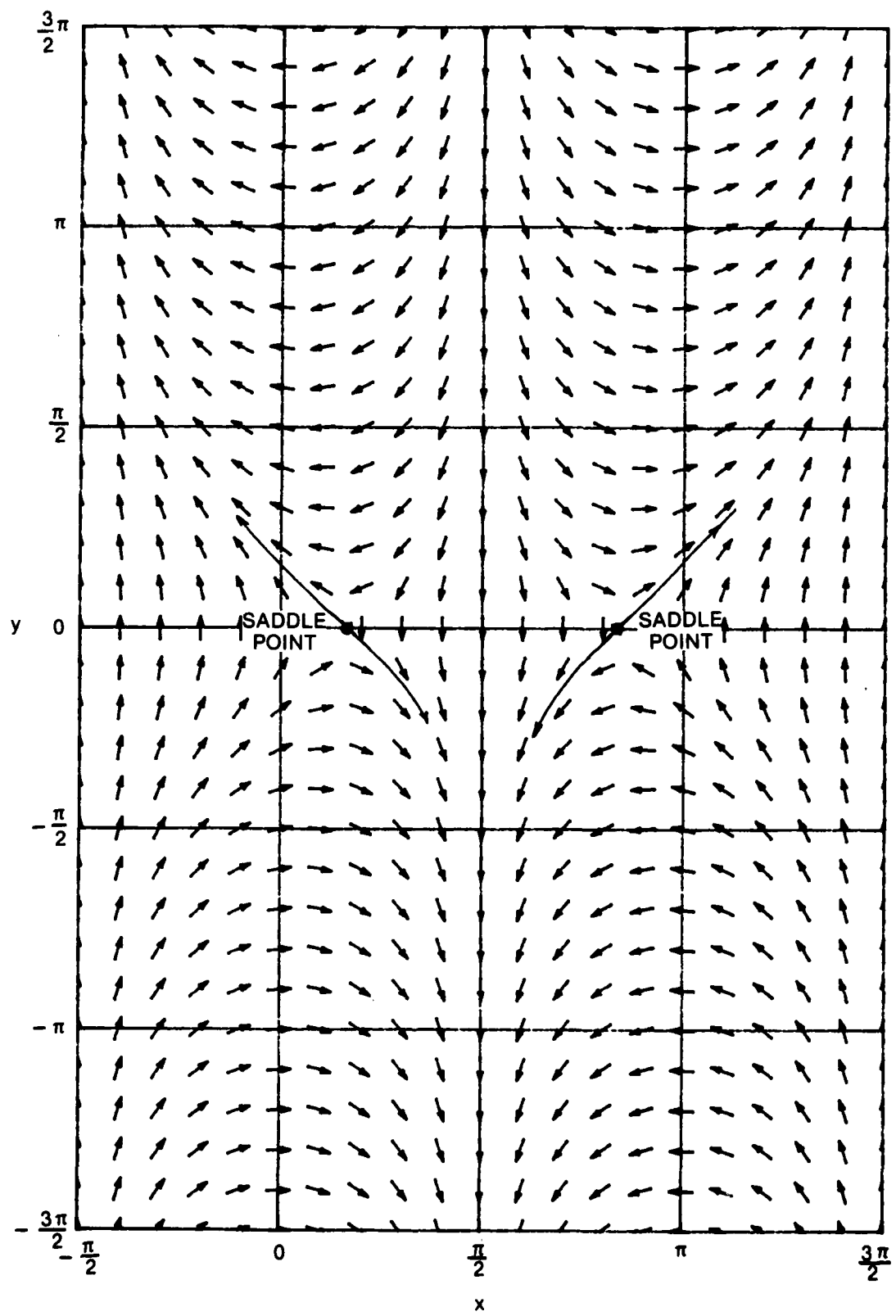
where the same square root branch must be taken as in (16).

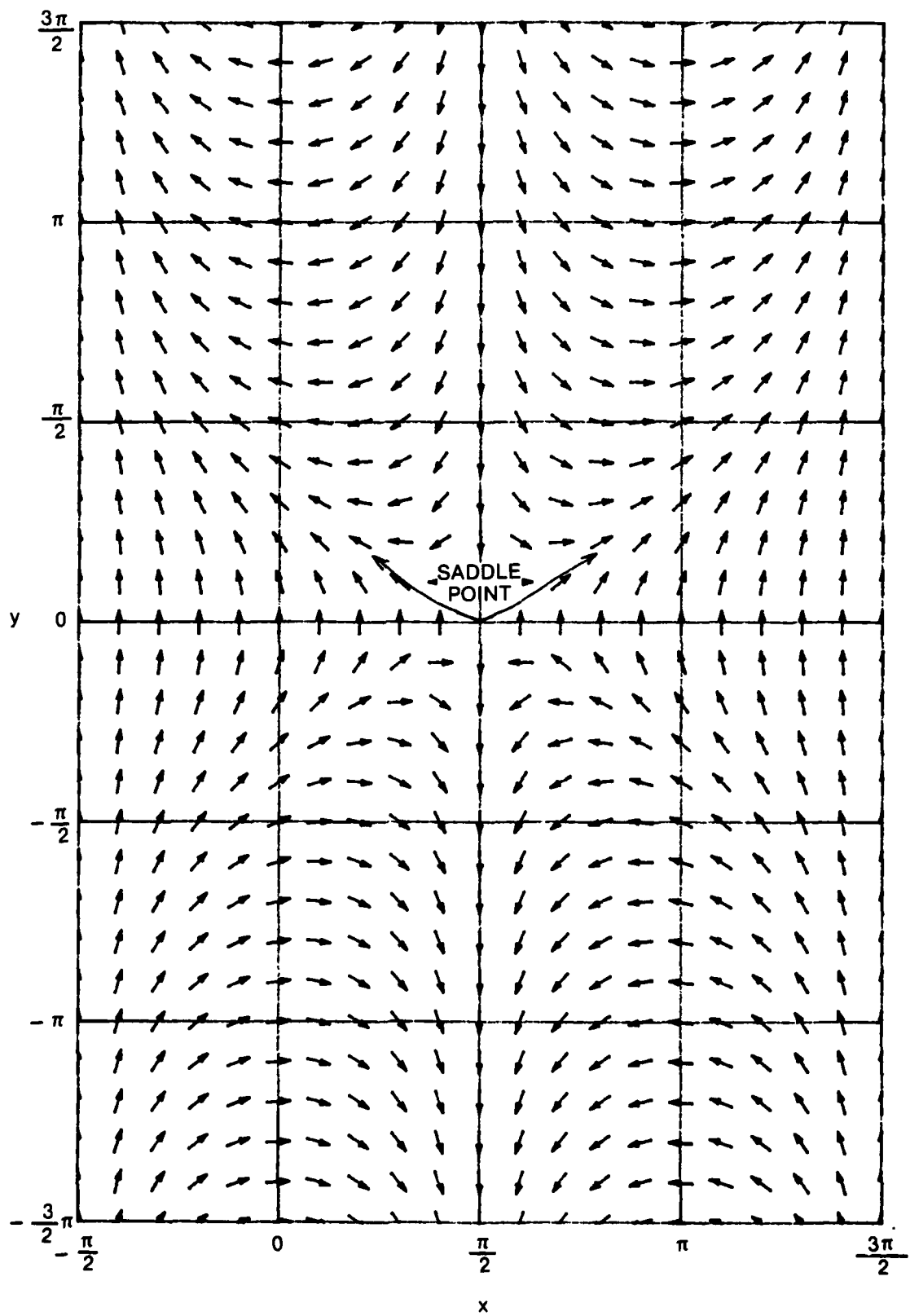
If one has available a computer program that evaluates the principal square root of a complex number, denoted here by  $z^{1/2}$ , it can be used to evaluate (17) in the following manner. Observe first that the branch line of principal square root  $z^{1/2}$  occurs where  $z = -p$  for  $p \geq 0$ ; i.e.,  $p$  can take on all nonnegative real values. So consider the representation

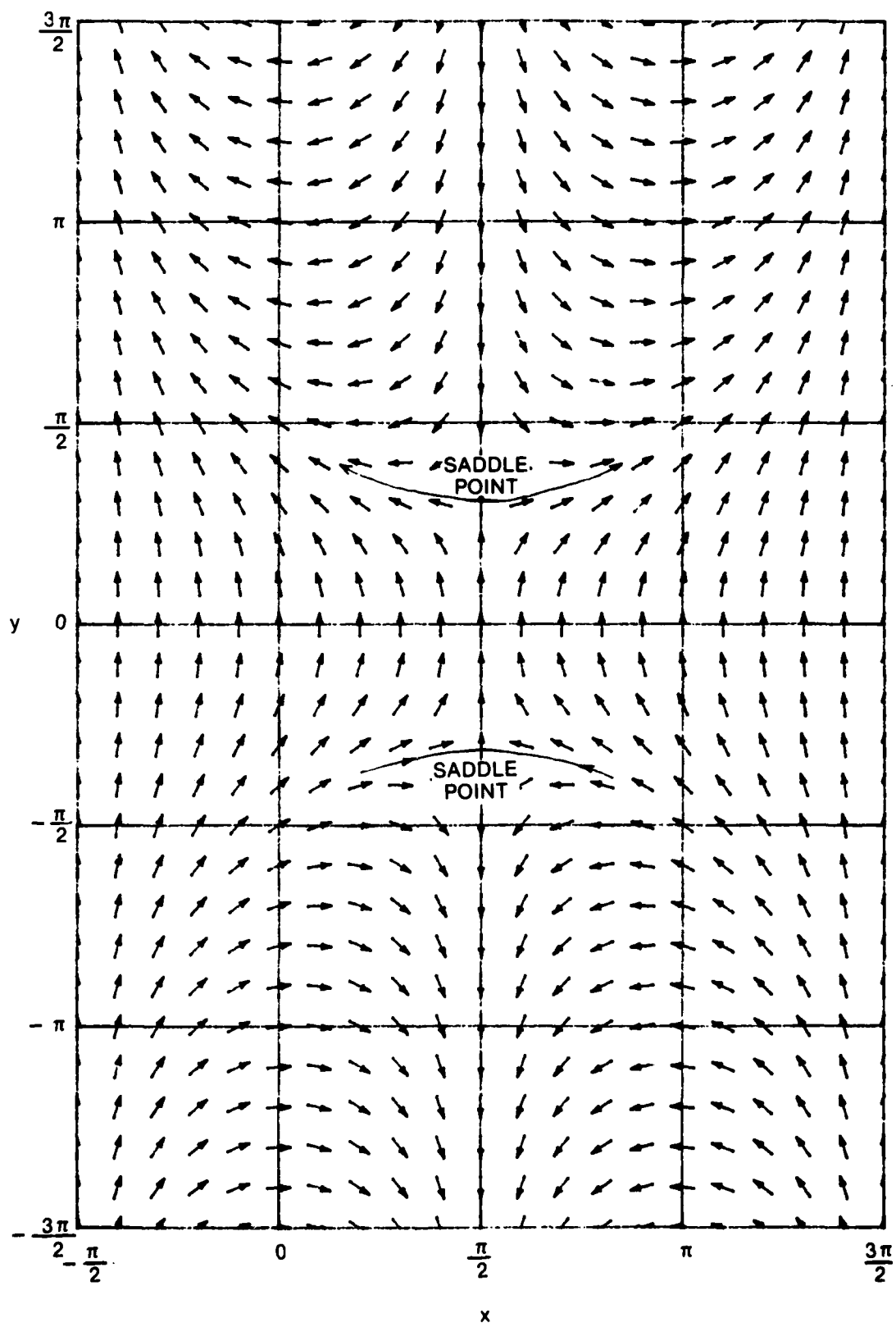
$$(z^2 - 1)\frac{1}{b}^{1/2} = i(-iz + i)^{1/2}(-iz - i)^{1/2}. \quad (18)$$

For  $z$  real, positive, and large, the right-hand side of (18) approaches  $i[\exp(-i\pi/4)z^{1/2}] [\exp(i\pi/4)z^{1/2}] = z$ , as desired. Furthermore, the two branch lines of (18) occur where the arguments of the two principal square roots have values

$$\begin{aligned} -iz \pm i &= -p \text{ for } p \geq 0; \\ \text{i.e., } z &= \pm 1 - ip \text{ for } p \geq 0. \end{aligned} \quad (19)$$

Figure 4. Steepest Descent Directions for Hankel Function,  $\beta = 0.5$

Figure 5. Steepest Descent Directions for Hankel Function,  $\beta = 1$

Figure 6. Steepest Descent Directions for Hankel Function,  $\beta = 1.5$

These are vertically downward from  $z = \pm 1$ , as desired. Thus (17) can be easily evaluated by taking the two complex principal square roots indicated in (18) and performing multiplication, division, and addition of complex numbers. The specific coding is illustrated in appendix A.

The pole of  $g(z)$  at  $z = v_0$  for this example (reference 1, 7.5.8) has no effect on the steepest descent contours of  $w(z)$ . The steepest descent directions for  $\theta = 0.8$  are depicted in figure 7. There are saddle points at  $z_s = \pm 5/3$ , and the steepest descent contours go vertically downward eventually. The steepest descent directions near the branch lines emanate from the branch lines themselves, but these branch lines have no effect on the steepest descent contours through the saddle points. However, if the branch line emanating from the branch point at  $z = 1$  had been taken at angle  $-\pi/6$ , for example, it would have interfered with the steepest descent contours in the 4th quadrant of the  $z$ -plane. Such a choice of branch for the square root in (16) and (17) is undesirable and should be avoided, as was done in figure 7.

### Function with Essential Singularity

This integrand is characterized by (reference 4)

$$\exp(w(z)) = z \exp\left(\frac{-K}{z-1}\right), \quad (20)$$

which function has a zero at  $z = 0$  and an essential singularity at  $z = 1$ . Then

$$\begin{aligned} w(z) &= \ln(z) - \frac{K}{z-1}, \\ w'(z) &= \frac{1}{z} + \frac{K}{(z-1)^2}. \end{aligned} \quad (21)$$

The steepest descent contours for (21) are depicted in figure 8 for  $K = 3$ . The essential singularity generates a "dipole effect" about  $z = 1$ , i.e., 0 at  $z = 1+$ , and  $\infty$  at  $z = 1-$ , for  $K > 0$ . The zero of (20) at  $z = 0$  manifests itself as a point toward which all the arrows point, since zero is the smallest magnitude that any complex function can take on. The saddle points (roots of (21)) occur at

$$z_s = \exp(\pm i\theta), \text{ where } \theta = \text{arc cos}\left(1 - \frac{K}{2}\right), \text{ for } 0 \leq K \leq 4. \quad (22)$$

Utilizing the information in figure 8, we find it relatively easy to decide what the effect of moving an original contour around in the  $z$ -plane will do to integral (1). Movement across the essential singularity at  $z = 1$  will necessitate consideration of the residue at this point. The zero and saddle points of (20) are not points of singularity.

### Cubic Function

This example comes from reference 3, pp. 296-302; it is characterized by  $g(z) = 1/2$  and (ibid., upper line of 6.6.25)

$$w(z) = -e^{i\alpha} \left(4z^2 - iz + \frac{1}{2}z^3\right). \quad (23)$$

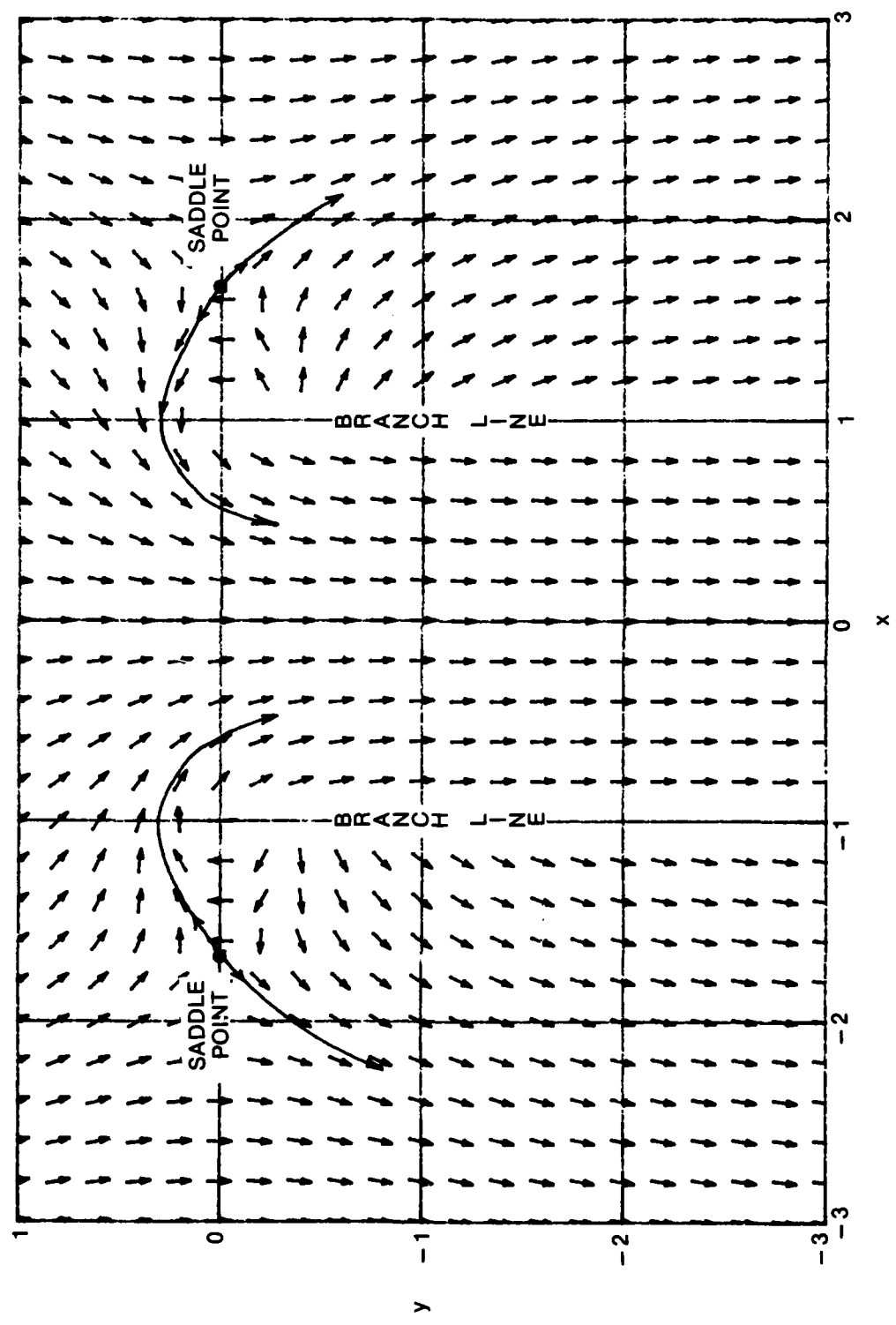


Figure 7. Steepest Descent Directions for Klein-Gordon Equation,  $\theta = 0.8$

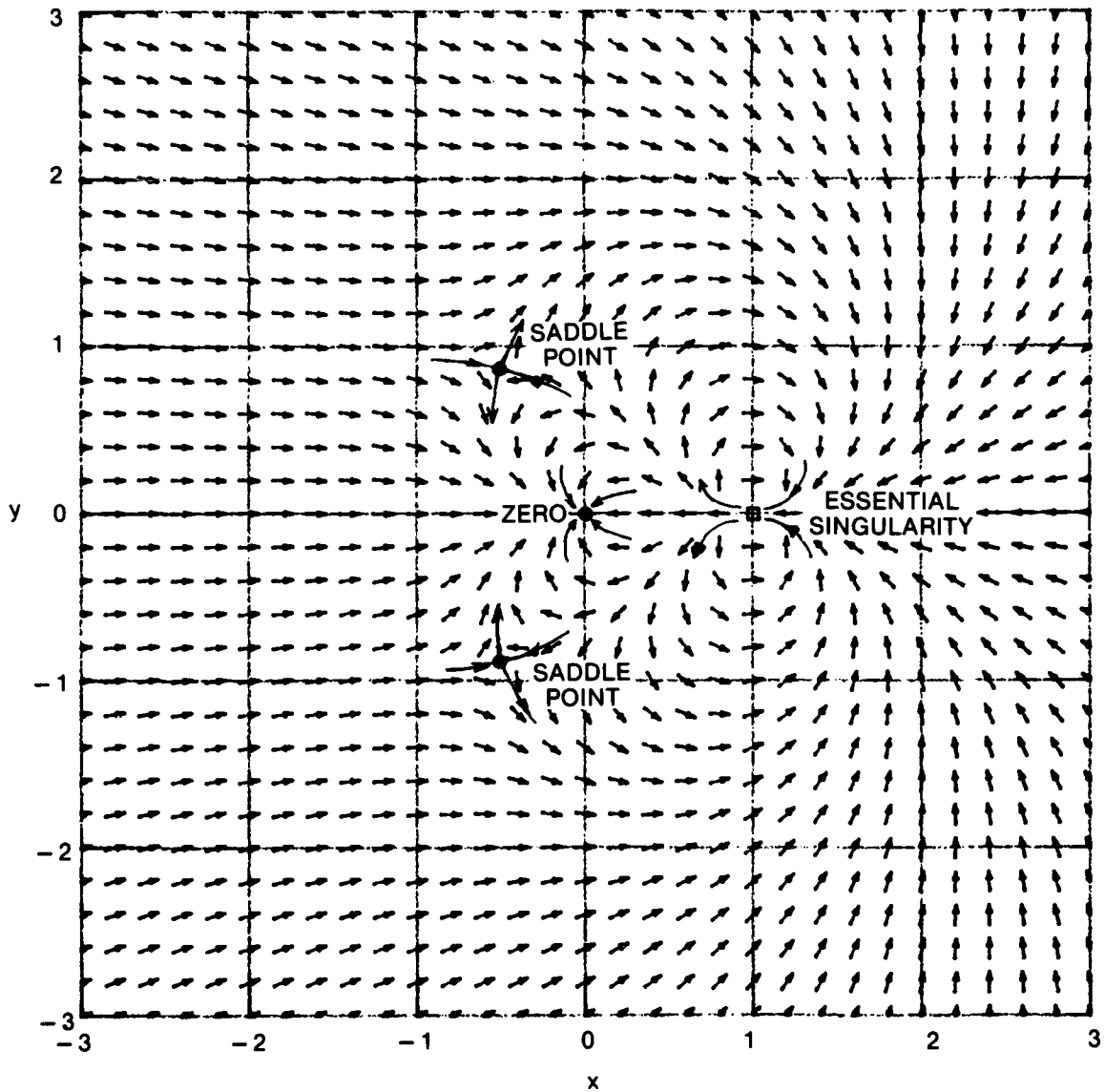


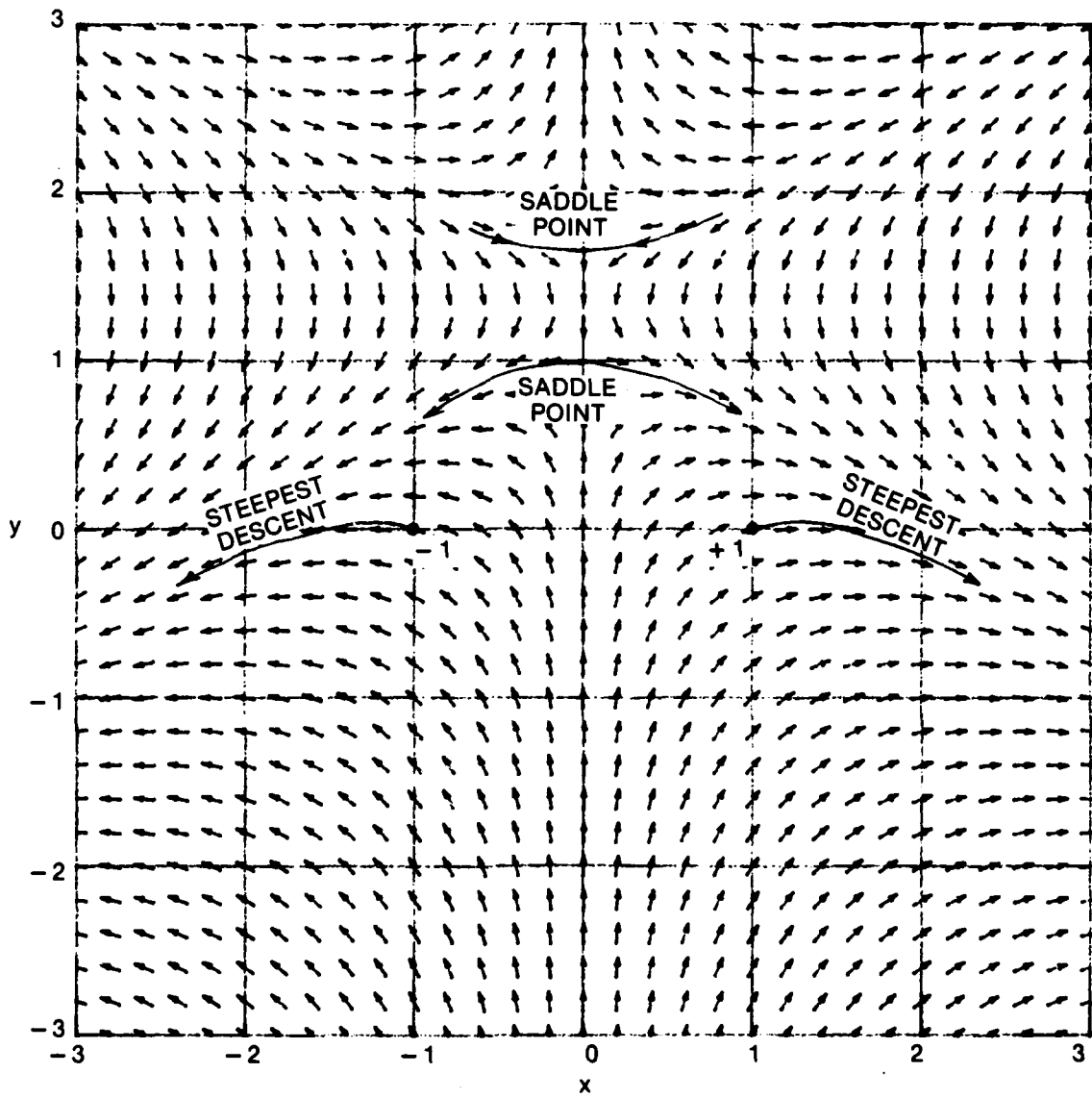
Figure 8. Steepest Descent Directions for  $w(z) = z \exp\left(\frac{-K}{z-1}\right)$ ,  $K = 3$

Also now the integral is a finite one, from  $z = -1$  to  $z = +1$ . This example exhibits a Stokes phenomenon at certain values of  $\alpha$ , where we have represented  $\lambda = |\lambda|e^{i\alpha}$ . We find

$$w'(z) = -e^{i\alpha} \left( 8z - i5 + i3z^2 \right), \quad (24)$$

which has zeros (saddle points) at  $z_s = i$  and  $i5/3$ .

A plot of steepest descent directions for  $\alpha = 0$  (positive real  $\lambda$ ) is given in figure 9. It indicates that the steepest descent contours out of the limits at  $z = -1, +1$  tend to  $\infty \exp(-i5\pi/6)$  and  $\infty \exp(-i\pi/6)$ , respectively. But these two valleys at  $\infty$  can be

Figure 9. Steepest Descent Directions for Cubic,  $\alpha = 0$ 

joined by the saddle point contribution through the point  $z_s = i$ . Thus the integral over  $(-1, 1)$  is exactly equal to the sum of these three steepest descent contours. The saddle point at  $z_s = i5/3$  need not be considered. The dominant contribution is obviously that at the saddle point  $z_s = i$ , as may be seen by the arrow directions.

For  $\alpha = 5\pi/12$ , figure 10 indicates a similar behavior. Since the steepest descent contours out of  $-1, +1$  tends to  $-175^\circ$  and  $-55^\circ$ , respectively, the saddle point at  $z_s = i$  must again be used to join them. The dominant contribution is seen to be due to  $z = -1$ , by making use of the arrows of descent in this figure.

For  $\alpha = 3\pi/4$ , however, we see from figure 11 that both of the steepest descent contours out of  $-1, +1$  tends to  $\infty \exp(-i5\pi/12)$ . Now there is no need to employ

either of the saddle points. The integral over  $(-1,1)$  is given exactly by the sum of the two steepest descent contributions. The dominant contribution is again due to  $z = -1$ , since we have to descend from  $z = -1$  to near  $z = 0$  to reach magnitude values comparable to those at  $z = +1$ .

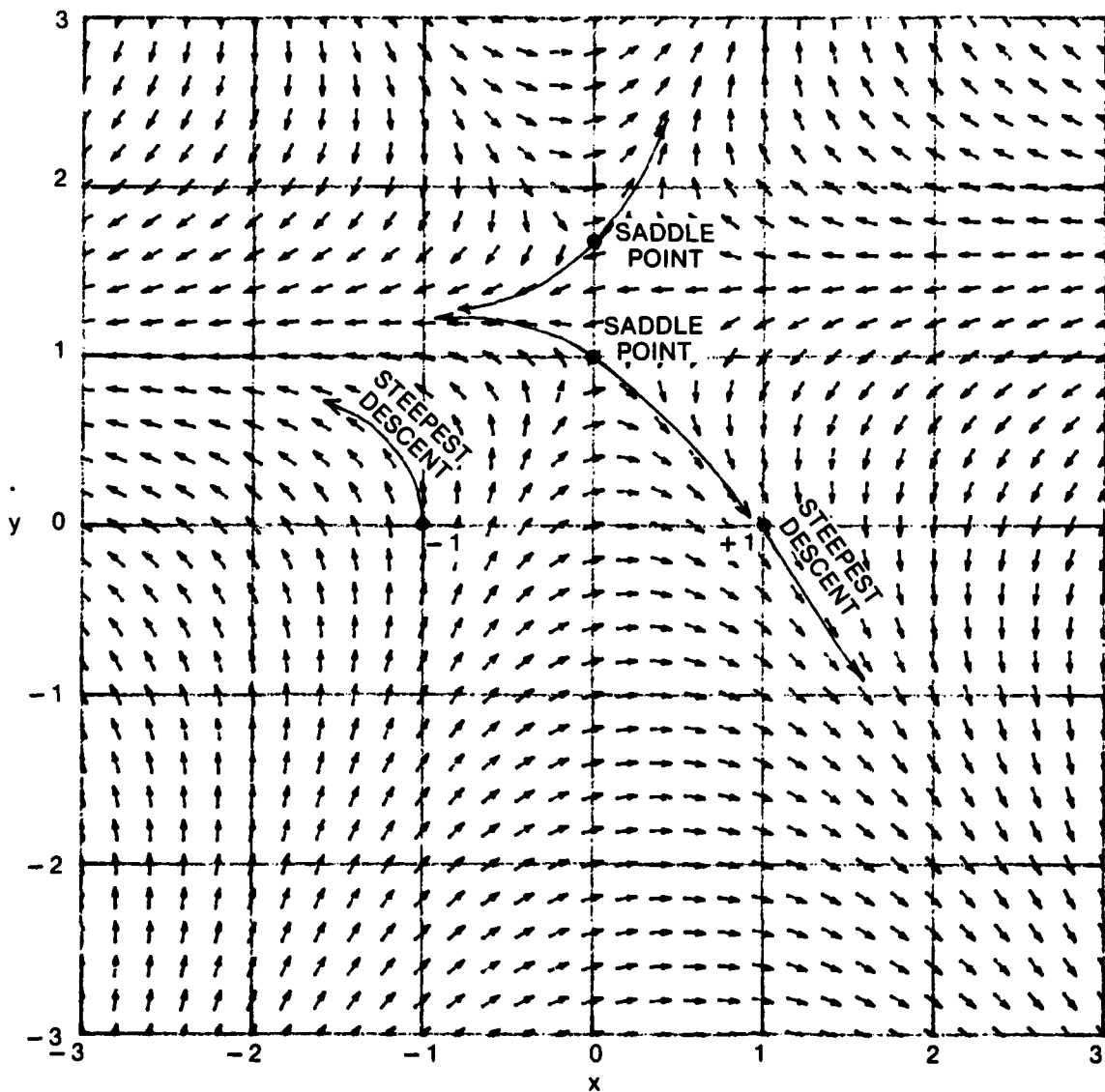


Figure 10. Steepest Descent Directions for Cubic,  $\alpha = 5\pi/12$

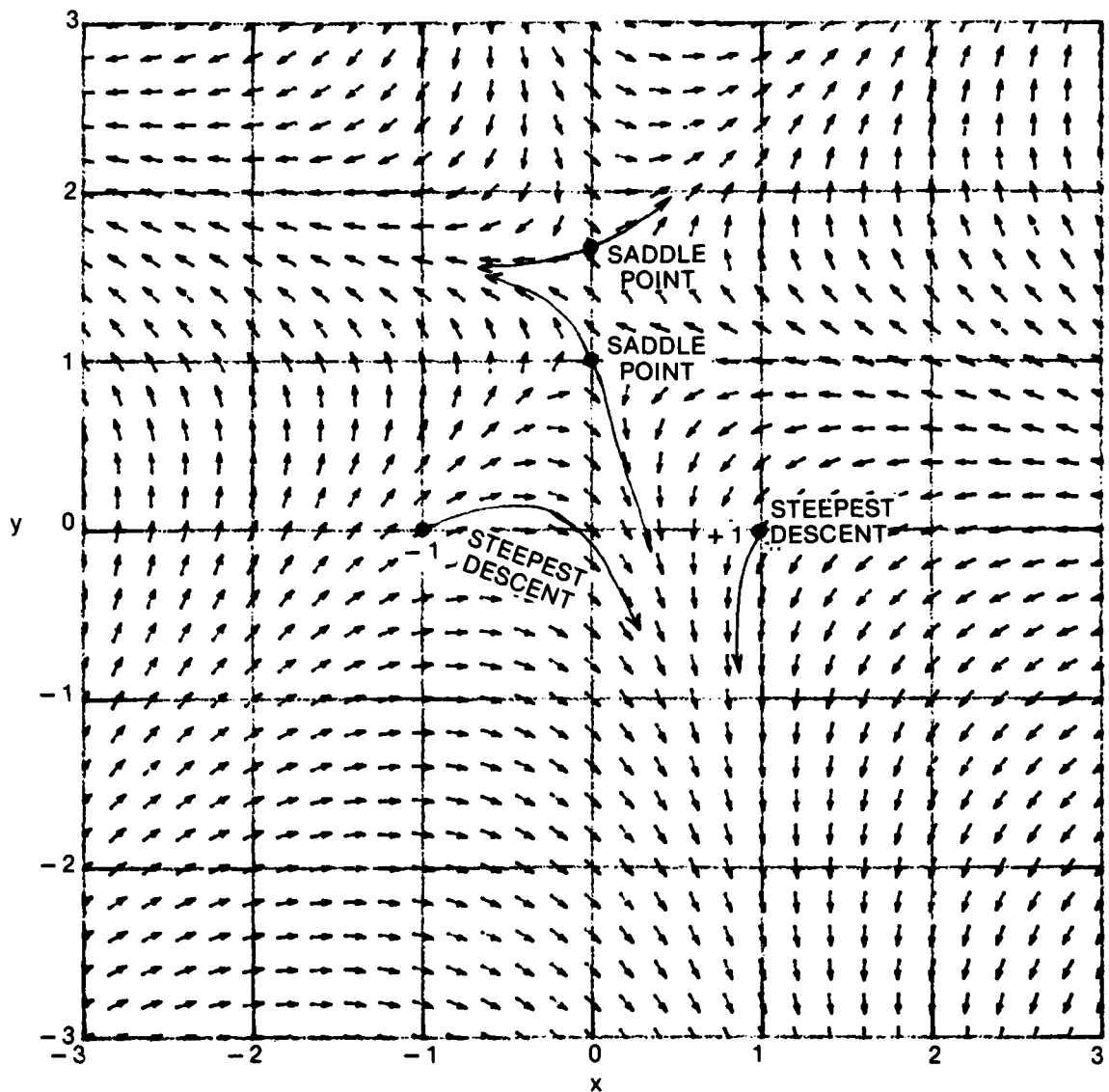


Figure 11. Steepest Descent Directions for Cubic,  $\alpha = 3\pi/4$

### Gaussian Exponent

The characteristic function of a particular type of impulsive noise is given in reference 5, equation (5), in the form

$$f(\xi) = \exp(-A) \sum_{m=0}^{\infty} \frac{A^m}{m!} \exp\left(-\frac{1}{2} \frac{mB_0^2}{2} \xi^2\right) \quad (25)$$

for a purely Poisson process (no Gaussian background). This summation can be evaluated in the closed form

$$f(\xi) = \exp\left(A \exp\left(-\frac{1}{2} \frac{B_0^2}{2} \xi^2\right) - A\right) . \quad (26)$$

The corresponding probability density function of this impulsive noise is given by the Fourier transform

$$p(v) = \frac{1}{2\pi} \int_{-\infty}^{+\infty} dz \exp\left(-izv + A \exp\left(-\frac{1}{2} \frac{B_0^2}{2} \xi^2\right) - A\right) . \quad (27)$$

By expanding  $f(\xi)$  in (26) in a power series, we note that the mean square value of the Poisson process is readily found to be  $AB_0^2/2$ . Since we will be interested in values for the dimensionless parameter  $A$  of the order of 1 (e.g.,  $A = 0.35$  in reference 5, figure 3), we will normalize our random variable according to  $t = v/(B_0^2/2)^{1/2} \equiv v/\sigma_0$ . Also, as,  $\xi \rightarrow \pm\infty$ ,  $f(\xi)$  in (26) tends to nonzero value  $\exp(-A)$ . Adding and subtracting this quantity and letting  $\xi = z/\sigma_0$  enables (27) to be expressed as

$$\begin{aligned} p(v) &= \exp(-A) \delta(v) \\ &+ \frac{\exp(-A)}{2\pi\sigma_0} \int_{-\infty}^{+\infty} dz \exp(-itz) [\exp(A \exp(-z^2/2)) - 1] . \end{aligned} \quad (28)$$

Although there is no obvious parameter  $\lambda$  in this form, it is shown in appendix B that we can still use steepest descent procedures on the logarithm of the integrand of (28); i.e., here we have

$$w(z) = -itz + \ln[\exp(a(z)) - 1] , \quad (29)$$

where we have defined

$$a(z) = A \exp(-z^2/2) . \quad (30)$$

Observe that as  $z \rightarrow \infty$  with  $\arg(z)$  in the two sectors within  $\pi/4$  of the positive-real or negative-real axes,  $a(z)$  becomes very small and

$$w(z) \sim -itz + \ln[a(z)] = -itz + \ln A - z^2/2 ; \quad (31)$$

this means that  $\operatorname{Re} w(z) \rightarrow -\infty$  in these two sectors of the  $z$ -plane, and, therefore, the integrand of (28) tends to zero in these sectors as  $z \rightarrow \infty$ .

The integrand of the integral of interest in (28) is zero in the finite  $z$ -plane only when

$$h(z_0) \equiv \exp(Ae^{-z_0^2/2}) - 1 = 0 ,$$

$$Ae^{-z_0^2/2} = i2\pi n \text{ for } n \neq 0 ,$$

$$-\frac{z_0^2}{2} = \ln\left(i \frac{2\pi n}{A}\right) + i2\pi m = \ln\left(\frac{2\pi|n|}{A}\right) + i\frac{\pi}{2} \operatorname{sgn}(n) + i2\pi m ,$$

$$z_0 = \pm i \left[ 2 \ln\left(\frac{2\pi|n|}{A}\right) + i\pi(4m + \operatorname{sgn}(n)) \right]^{1/2} , \quad (32)$$

where  $A > 0$ , the square root is the principal branch, and  $n$  and  $m$  are arbitrary integers (negative, zero, or positive), except that  $n \neq 0$ . These zeros of  $h(z)$  are important because they will be locations toward which all the steepest descent arrows must point in their neighborhoods, since zero is the smallest magnitude that a complex function can take on. These zero locations, of which there are an infinite number, depend only on  $A$ , and not on normalized variable  $t = v/\sigma_0$  in expression (28) for the probability density  $p(v)$ . The locations of the zeros of  $h(z)$  in the third quadrant closest to the origin are depicted in figure 12 for  $A = 0.35$ . There is symmetry in the other quadrants since (from the first line of (32))

$$h(-z) = h(z) , \quad h(z^*) = h^*(z) . \quad (33)$$

For purposes of evaluating steepest descent directions and saddle point locations, we note that  $a(z)$  in (30) has the property

$$a'(z) = -za(z) , \quad (34)$$

and so (29) yields

$$w'(z) = -it - \frac{z a(z)}{1 - \exp(-a(z))} . \quad (35)$$

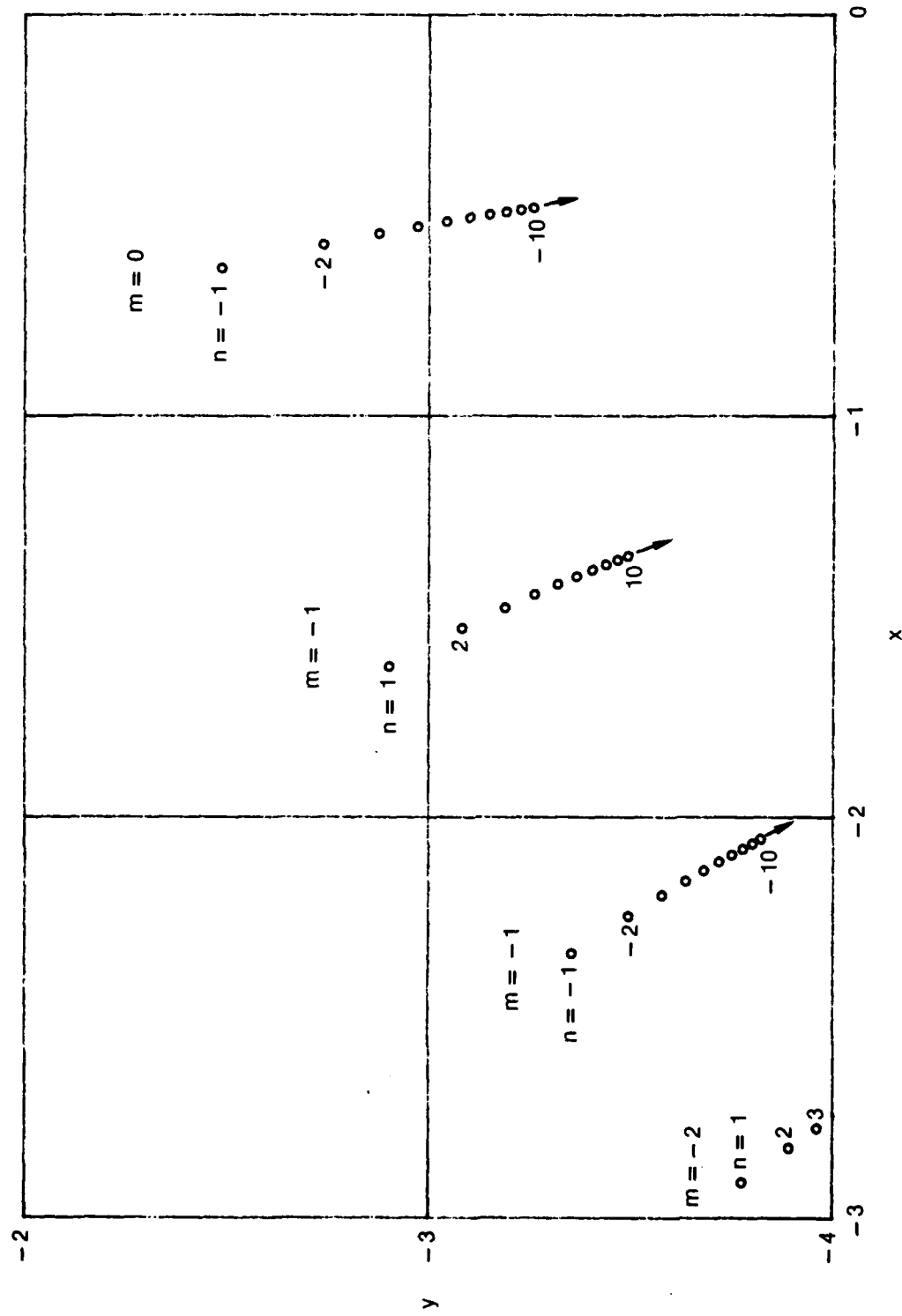
Thus the saddle points,  $z_s$ , of which there are an infinite number, are solutions of

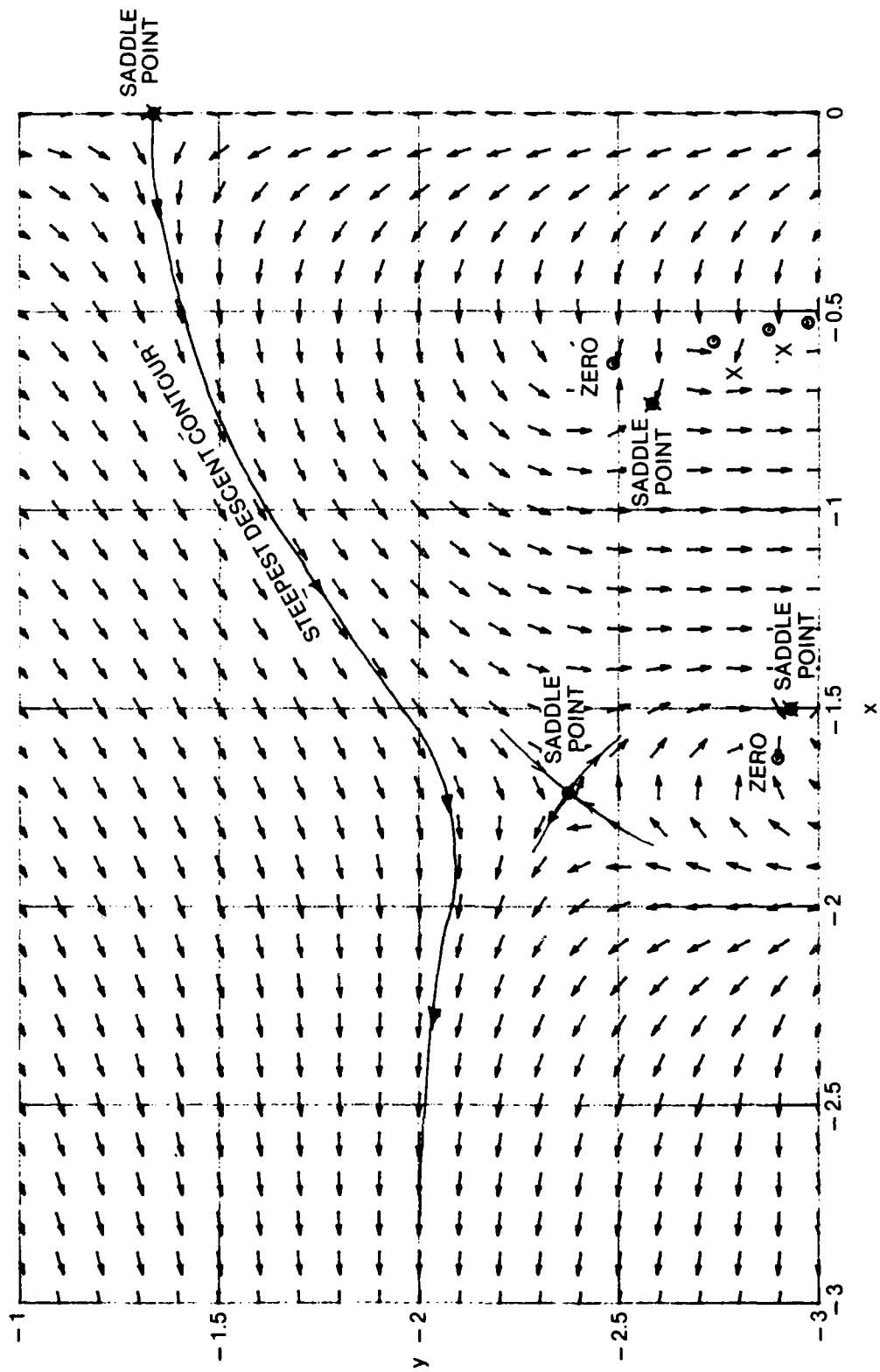
$$\frac{z_s a(z_s)}{1 - \exp(-a(z_s))} = -it , \quad (36)$$

and obviously depend on both  $A$  and  $t$ . The most important saddle point is at  $z_s = -i\beta$ ,  $\beta$  positive real, where (using (30)),

$$\frac{\beta A \exp(\beta^2/2)}{1 - \exp(-A \exp(\beta^2/2))} = t . \quad (37)$$

The steepest descent directions for  $A = 0.35$ ,  $t = 2$  are depicted for (35) in figure 13. The saddle point at  $z_s = -i\beta = -i1.341$  satisfies (37); there are five other saddle points indicated by  $\times$  in the figure, in addition to the zeros carried over from figure 12. The steepest descent contour out of the saddle point  $z_s = -i1.341$  is drawn as a solid line; it is asymptotic to  $y = -t$  as  $z \rightarrow \infty$  with  $\arg(z)$  within  $\pi/4$  of the positive- and negative-real axes. Movement of the original contour from the real axis in (28) to the steepest descent contour is easily justified.

Figure 12. Zero Locations for  $A = 0.35$

Figure 13. Steepest Descent Contour for  $A = 0.35, t = 2$

To deduce the asymptotic nature of the steepest descent contours, recall (31); thus the imaginary part of  $w$  is

$$v \sim -tx - xy = -x(y + t) \text{ as } z \rightarrow \infty \quad (38)$$

in the sectors under consideration. But, since from (29),

$$w(-i\gamma) = -\gamma t + \ln[\exp(\lambda \exp(\gamma^2/2)) - 1] \quad (39)$$

is real, we require (38) to approach 0 as  $x \rightarrow \pm\infty$ . This requires that  $y \rightarrow -t$ , as claimed.

We observe from figure 13 that no use is made of the saddle point at  $(-1.71, -2.38)$ , nor of the infinite number of other saddle points. We also observe that the descent directions in the neighborhood of the closely spaced zeros and saddle points near the bottom of the figure is very detailed and complicated; however, none of that information is needed.

When  $t$  is increased to 5, figure 14 applies. Now the steepest descent contour out of the saddle point at  $z_s = -i\beta = -i1.945$  heads into the zero at  $(-0.632, -2.485)$ . How to connect from this latter point to  $z = -\infty$  is not clear. Instead, we consider a horizontal descent contour out of  $z_s = -i1.945$  until we get in the neighborhood of  $(-2, -2)$ , and then we resume a steepest descent contour heading toward  $y = -t = -5$ . The major contribution to this descent contour is given by the neighborhood of the saddle point at  $x = 0$ ; the descent and steepest descent contours are tangent at this saddle point.

The aid afforded by the steepest descent directions depicted in figures 13 and 14 is extremely worthwhile, since the exponential in (29) and (35) makes an analytical approach very difficult. The ability to discard or avoid certain regions of the  $z$ -plane in determining an appropriate descent contour is rather obvious from the figures when coupled with basic information about the integrand, like the asymptotic behavior of the steepest descent contour.

The above results yield exact values for the original integral, since we have simply determined contours equivalent to those originally specified. Now we will derive an asymptotic expansion for the probability density in (28) for large  $t = v/\sigma_0$ , i.e., at values  $v$  much larger than the standard deviation of the Poisson process.

To do this, we need

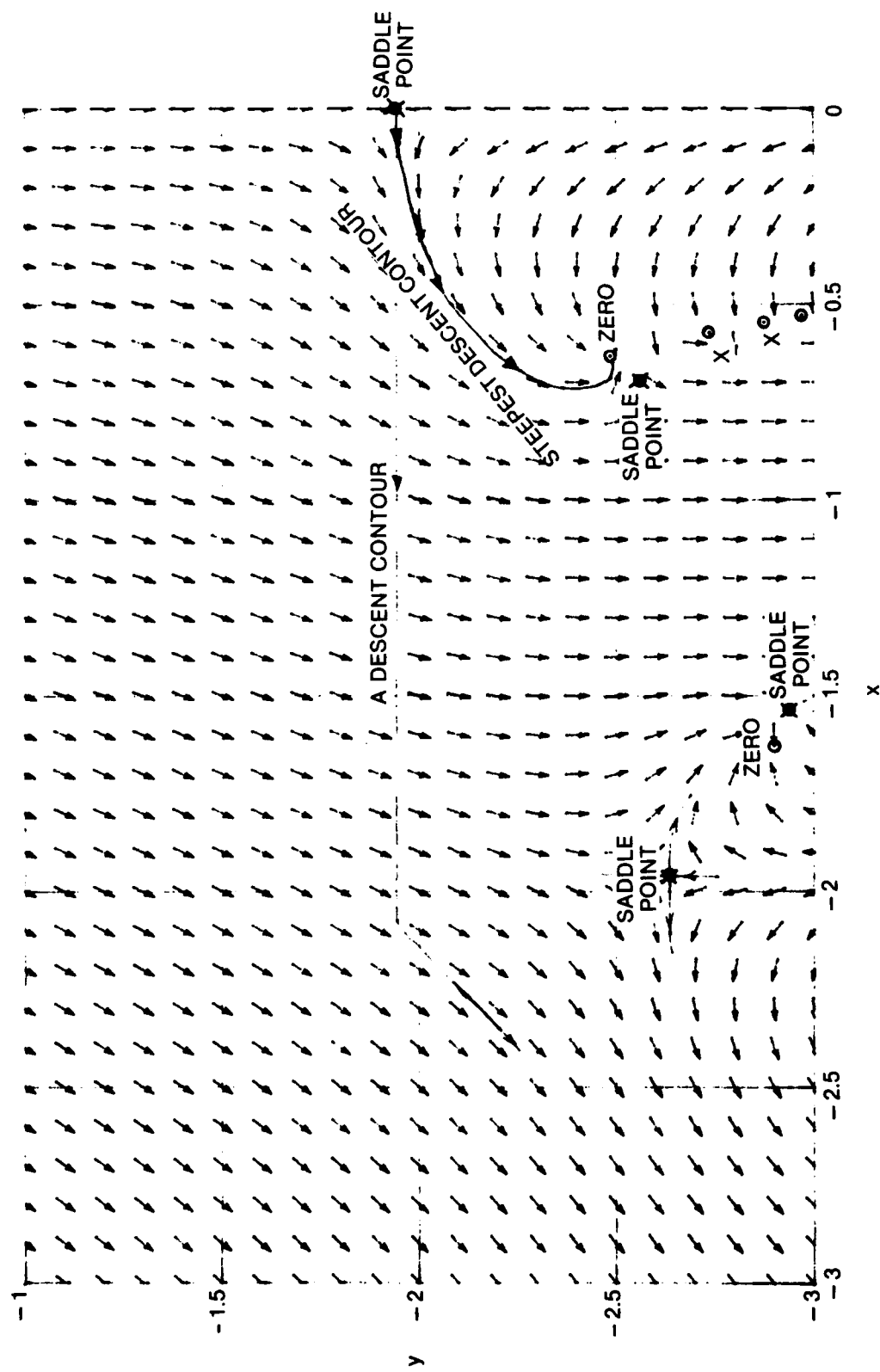
$$w''(z) = a(1 - e^{-a})^{-2} \left[ z^2 - 1 + e^{-a} (1 - z^2 - z^2 a) \right], \quad (40)$$

where  $a = a(z)$  is defined in (30). Then we find

$$w''(z_s) = t^2 + i \frac{t}{z_s} (1 - z_s^2 - z_s^2 a(z_s)) \quad (41)$$

and, in particular,

$$w''(-i\beta) = t^2 - \frac{t}{\beta} (1 + \beta^2 + \beta^2 \lambda \exp(\beta^2/2)), \quad (42)$$

Figure 14. Descent Contours for  $A = 0.35, t = 5$

for the saddle point at  $z_s = -i\beta$ . Also  $w(-i\beta)$  is given by (39). Then we have the approximation (reference 1, chapter 7)

$$p(v) \sim \frac{\exp(-A - \beta t)}{2\pi\sigma_0} \left[ \exp\left(A \exp(\beta^2/2)\right) - 1 \right] \left( \frac{2\pi}{|w'(-i\beta)|} \right)^{1/2} \text{ as } t \rightarrow +\infty . \quad (43)$$

One drawback with this solution is that  $\beta$  depends on  $t$  through the solution of transcendental equation (37). For large  $t$ , we have, to first order,

$$\beta \approx [2 \ln(t/A)]^{1/2} \approx L^{1/2} . \quad (44)$$

For development of additional terms and the general philosophy of solution of these types of problems, see reference 6, pp. 11-16 and 83-84. We find, more generally,

$$\beta^2 \approx L - \frac{L}{L+1} \ln(L) . \quad (45)$$

Even so, substitution into (43) yields a very complicated expression for the probability density function unless  $t$  is excessively large. It can be seen that (43) decays slightly faster than an exponential for large  $t$ .

### Summary

A technique for simple determination of the steepest descent direction at any point in the complex plane has been presented and illustrated with numerous examples. The movement of the original contour to an equivalent descent or steepest descent contour is an exact representation and can be deduced fairly easily from the descent information. At this point, two alternatives are available, either exact numerical evaluation of the integral or an approximation such as Laplace's method. Very difficult integrands can be handled very effectively via this approach.

## Appendix A

### Computer Programs

The major part of the calculations required for the six examples in the main text is that of  $w'(z)$ . This is accomplished in the Subroutine Wderivative in the main program written in BASIC and listed at the end of this appendix. But, first, the six subroutines for the examples given are listed. They illustrate how little programming is actually needed to compute  $w'(z)$ , provided that one has already written subroutines for the standard complex operations and functions like multiply, divide,  $\exp(z)$ ,  $\log(z)$ , square root,  $\arg(z)$ ,  $\sin(z)$ ,  $\cos(z)$ , etc. These latter functions are listed for completeness as subroutines at the end of the enclosed program.

```

410  SUB Wderivative(X,Y,Rew1,Imw1)      ! Airy function
411  COM Ct,St                         ! cos(theta), sin(theta)
412  CALL Mul(X,Y,X,Y,A,B)
420  Rew1=Ct-A
430  Imw1=St-B
440  SUBEND

410  SUB Wderivative(X,Y,Rew1,Imw1)      ! Hankel function
411  Beta=.5
412  CALL Sin(X,Y,A,B)
420  Rew1=B
430  Imw1=Beta-A
440  SUBEND

410  SUB Wderivative(X,Y,Rew1,Imw1)      ! Klein-Gordon
411  Theta=.8
412  CALL Sqr(Y,-X+1,A,B)
413  CALL Sqr(Y,-X-1,C,D)
414  CALL Mul(A,B,C,D,E,F)
415  CALL Div(Theta*X,Theta*Y,E,F,G,H)
420  Rew1=G
430  Imw1=H-1
440  SUBEND

410  SUB Wderivative(X,Y,Rew1,Imw1)      ! Essential singularity
411  K=3
412  CALL Mul(X-1,Y,X-1,Y,A,B)
413  CALL Div(K,0,A,B,C,D)
414  CALL Div(1,0,X,Y,E,F)
420  Rew1=C+E
430  Imw1=D+F
440  SUBEND

```

TR 6433

```
410  SUB Wderivative(X,Y,Rew1,Imw1)      ! cubic function
411  COM Ca,Sa                         ! cos(alpha), sin(alpha)
412  CALL Mul(X,Y,X,Y,A,B)
413  CALL Mul(Ca,Sa,8*X-3*B,8*Y-5+3*A,C,D)
420  Rew1=-C
430  Imw1=-D
440  SUBEND
```

```
410  SUB Wderivative(X,Y,Rew1,Imw1)      ! Gaussian exponent
411  R=.35
412  T=2
413  CALL Mul(X,Y,X,Y,T1,T2)
414  CALL Exp(-.5*T1,-.5*T2,T3,T4)
415  Ar=R*T3
416  Ai=R*T4
417  CALL Exp(-Ar,-Ai,Er,Ei)
418  CALL Mul(X,Y,Ar,Ai,T1,T2)
419  CALL Div(T1,T2,1-Er,-Ei,T3,T4)
420  Rew1=-T3
430  Imw1=-T-T4
440  SUBEND
```

```

1 ! Steepest Descent via w'(z); use SUB Wderivative in line 410
10  X1=-3                      ! LEFT ABSCISSA
20  X2=3                      ! RIGHT ABSCISSA
30  Y1=-3                      ! BOTTOM ORDINATE
40  Y2=3                      ! TOP ORDINATE
50  Dx=.2                      ! X INCREMENT
60  Dy=.2                      ! Y INCREMENT
70  PLOTTER IS "GRAPHICS"
80  GRAPHICS
90  SCALE X1,X2,Y1,Y2
100 LINE TYPE 3
110 GRID 1,1                   ! GRID LINE SPACING
120 LINE TYPE 1
130 F=.2*SQR(Dx*Dx+Dy*Dy)    ! ARROW
140 Q1=1-COS(PI/12)*.8        ! INFOR-
150 Q2=SIN(PI/12)*.8          ! MATION
160 FOR X=X1 TO X2 STEP Dx
170 FOR Y=Y1 TO Y2 STEP Dy
180 CALL Wderivative(X,Y,Rew1,Imw1) ! w'(z)
190 CALL Direction(Rew1,Imw1,Cos,Sin) ! direction of steepest descent
200 IF ABS(Cos)+ABS(Sin)>0 THEN 230
210 OUTPUT 0;"SADDLE POINT AT ";X;Y
220 GOTO 350
230 T1=F*Cos
240 T2=F*Sin
250 Xa=X+T1*Q1
260 Xb=T2*Q2
270 Ya=Y+T2*Q1
280 Yb=T1*Q2
290 MOVE X-T1,Y-T2
300 DRAW X+T1,Y+T2
310 MOVE Xa+Xb,Ya-Yb
320 DRAW X+T1,Y+T2
330 DRAW Xa-Xb,Ya+Yb
340 PENUP
350 NEXT Y
360 NEXT X
370 PAUSE
380 DUMP GRAPHICS
390 END
400 !
410 SUB Wderivative(X,Y,Rew1,Imw1) ! Riny function
420 Rew1=1-X*X+Y*Y               ! w(z)=z-z^3-3
430 Imw1=-2*X*Y                 ! w'(z)=1-z^2
440 SUBEND
450 !
460 SUB Direction(Rew1,Imw1,Cos,Sin) ! direction of
470 T=SQR(Rew1*Rew1+Imw1*Imw1)    ! steepest descent
480 IF T>0 THEN 510
490 Cos=Sin=0
500 GOTO 530
510 Cos=-Rew1/T
520 Sin=Imw1/T
530 SUBEND
540 !

```

## TR 6433

```

550  SUB Mul(X1,Y1,X2,Y2,A,B)      ! Z1*Z2
560  A=X1*X2-Y1*Y2
570  B=X1*Y2+X2*Y1
580  SUBEND
590  !
600  SUB Div(X1,Y1,X2,Y2,A,B)      ! Z1/Z2
610  T=X2*X2+Y2*Y2
620  A=(X1*X2+Y1*Y2)/T
630  B=(Y1*X2-X1*Y2)/T
640  SUBEND
650  !
660  SUB Exp(X,Y,A,B)            ! EXP(Z)
670  T=EXP(X)
680  A=T*COS(Y)
690  B=T*SIN(Y)
700  SUBEND
710  !
720  SUB Log(X,Y,A,B)          ! PRINCIPAL LOG(Z)
730  A=.5*LOG(X*X+Y*Y)
740  IF X<>0 THEN 770
750  B=.5*PI*SGN(Y)
760  GOTO 790
770  B=ATN(Y/X)
780  IF X<0 THEN B=B+PI*(1-2*(Y<0))
790  SUBEND
800  !
810  SUB Sqr(X,Y,A,B)          ! PRINCIPAL SQR(Z)
820  IF X<>0 THEN 860
830  A=B=SQR(.5*ABS(Y))
840  IF Y<0 THEN B=-B
850  GOTO 970
860  F=SQR(SQR(X*X+Y*Y))
870  T=.5*ATN(Y/X)
880  A=F*COS(T)
890  B=F*SIN(T)
900  IF X>0 THEN 970
910  T=A
920  A=-B
930  B=T
940  IF Y>=0 THEN 970
950  A=-A
960  B=-B
970  SUBEND
980  !
990  SUB Arg(X,Y,A)            ! PRINCIPAL ARG(Z)
1000  IF X=0 THEN A=.5*PI*SGN(Y)
1010  IF X<>0 THEN A=ATN(Y/X)
1020  IF X<0 THEN A=A+PI*(1-2*(Y<0))
1030  SUBEND
1040  !
1050  SUB Power(X,Y,R,A,B) ! PRINCIPAL POWER Z^R
1060  F=EXP(.5*R*LOG(X*X+Y*Y))
1070  CALL Arg(X,Y,T)
1080  A=F*COS(R*T)
1090  B=F*SIN(R*T)
1100  SUBEND
1110  !

```

```

1120  SUB Sin(X,Y,A,B)          ! SIN(Z)
1130  E=EXP(Y)
1140  A=.5*SIN(X)*(E+1/E)
1150  IF ABS(Y)<.1 THEN 1180
1160  S=.5*(E-1/E)
1170  GOTO 1200
1180  S=Y*Y
1190  S=Y*(120+S*(20+S))/120
1200  B=COS(X)*S
1210  SUBEND
1220  !
1230  SUB Cos(X,Y,A,B)          ! COS(Z)
1240  E=EXP(Y)
1250  A=.5*COS(X)*(E+1/E)
1260  IF ABS(Y)<.1 THEN 1290
1270  S=.5*(E-1/E)
1280  GOTO 1310
1290  S=Y*Y
1300  S=Y*(120+S*(20+S))/120
1310  B=-SIN(X)*S
1320  SUBEND
1330  !
1340  SUB Sinh(X,Y,A,B)         ! SINH(Z)
1350  E=EXP(X)
1360  B=.5*SIN(Y)*(E+1/E)
1370  IF ABS(X)<.1 THEN 1400
1380  S=.5*(E-1/E)
1390  GOTO 1420
1400  S=X*X
1410  S=X*(120+S*(20+S))/120
1420  A=COS(Y)*S
1430  SUBEND
1440  !
1450  SUB Cosh(X,Y,A,B)         ! COSH(Z)
1460  E=EXP(X)
1470  A=.5*COS(Y)*(E+1/E)
1480  IF ABS(X)<.1 THEN 1510
1490  S=.5*(E-1/E)
1500  GOTO 1530
1510  S=X*X
1520  S=X*(120+S*(20+S))/120
1530  B=SIN(Y)*S
1540  SUBEND

```

## Appendix B

### Steepest Descent for General Analytic Function

Here we do not force the integrand to be of the form in (1), but consider the general integral  $\int_C dz f(z)$ . Let  $f(z)$  be analytic in a region in the complex plane. The magnitude-squared value is

$$M = |f(z)|^2 \equiv f_r^2 + f_i^2 . \quad (B-1)$$

The direction of steepest descent for  $M$  is opposite to the gradient of  $M$ , which is

$$\nabla M = \frac{\partial M}{\partial x} \hat{a}_x + \frac{\partial M}{\partial y} \hat{a}_y . \quad (B-2)$$

But, from (B-1),

$$\begin{aligned} \frac{\partial M}{\partial x} &= 2 \left( f_r \frac{\partial f_r}{\partial x} + f_i \frac{\partial f_i}{\partial x} \right) , \\ \frac{\partial M}{\partial y} &= 2 \left( f_r \frac{\partial f_r}{\partial y} + f_i \frac{\partial f_i}{\partial y} \right) . \end{aligned} \quad (B-3)$$

Now if function  $f$  is analytic at  $z$ , then

$$f'(z) = \frac{\partial f_r}{\partial x} + i \frac{\partial f_i}{\partial x} = \frac{\partial f_i}{\partial y} - i \frac{\partial f_r}{\partial y} . \quad (B-4)$$

So we can express

$$\begin{aligned} \frac{\partial M}{\partial x} &= 2 \operatorname{Re}\{f^*(z) f'(z)\} , \\ \frac{\partial M}{\partial y} &= -2 \operatorname{Im}\{f^*(z) f'(z)\} . \end{aligned} \quad (B-5)$$

Therefore, the steepest descent direction for  $M$  has components that are the negatives of (B-5) or, equivalently, are proportional to

$$-\operatorname{Re} \left\{ \frac{f'(z)}{f(z)} \right\} , \quad \operatorname{Im} \left\{ \frac{f'(z)}{f(z)} \right\} . \quad (B-6)$$

The basic calculation for determination of steepest descent directions is thus seen to be

$$f'(z)/f(z) = \frac{d}{dz} \ln f(z).$$

When  $f'(z_s) = 0$ , we have a saddle point of  $f$  at  $z = z_s$ . Near the saddle point,

$$f(z) \approx f(z_s) + \frac{1}{2} f''(z_s) (z - z_s)^2 \approx f_0 + \frac{1}{2} f_2 \Delta^2 \text{ for small } \Delta . \quad (B-7)$$

Then

$$\begin{aligned} M &\equiv \left( f_0 + \frac{1}{2} f_2 \Delta^2 \right) \left( f_0^* + \frac{1}{2} f_2^* \Delta^2 \right) \\ &\equiv |f_0|^2 + \operatorname{Re} \left\{ f_0^* f_2 \Delta^2 \right\} \text{ for small } \Delta . \end{aligned} \quad (B-8)$$

Now let

$$f_0^* f_2 = a e^{i\alpha}, \quad \Delta = r e^{i\theta} . \quad (B-9)$$

Then (B-8) yields

$$M \equiv |f_0|^2 + a r^2 \cos(\alpha + 2\theta) , \quad (B-10)$$

which has two peaks and two valleys versus  $\theta$  in a  $2\pi$  interval (for  $a \neq 0$ ); this is characteristic of a saddle point. The directions of steepest descent,  $\theta_d$ , at  $z = z_s$  occur when

$$\alpha + 2\theta_d = \pi \text{ or } 3\pi, \quad \theta_d = \frac{\pi - \alpha}{2} \text{ or } \frac{\pi - \alpha}{2} + \pi . \quad (B-11)$$

Notice, from (B-9), that

$$\alpha = \arg \left\{ f_0^* f_2 \right\} = \arg \left\{ f^*(z_s) f''(z_s) \right\} = \arg \left\{ f''(z_s) / f(z_s) \right\} . \quad (B-12)$$

Now let us investigate the behavior of the complex function  $f(z)$  near  $z_s$ , along the steepest descent contours. For  $\theta_d$  as given by (B-11),  $\Delta$  in (B-9) becomes

$$\Delta = \pm r \exp \left( i \frac{\pi - \alpha}{2} \right), \quad \Delta^2 = -r^2 e^{-i\alpha} ; \quad (B-13)$$

and there follows, from (B-7) and (B-9), for small  $r$ ,

$$\begin{aligned} f(z) &\equiv f_0 - \frac{1}{2} r^2 f_2 e^{-i\alpha} = f_0 \left( 1 - \frac{r^2 a}{2 |f_0|^2} \right) \\ &\text{on steepest descent contour near } z_s . \end{aligned} \quad (B-14)$$

That is, since the term in parentheses is real and positive,

$$\arg f(z) = \arg f(z_s) \text{ on steepest descent contour near } z_s . \quad (B-15)$$

More generally, it can be shown that

$$\arg f(z) = \arg f(z_s)$$

everywhere on steepest descent contour through  $z_s$ . (B-16)

Now let us apply these general results to the special case where  $f(z) = \exp(w(z))$ . Then  $f'(z) = w'(z) \exp(w(z))$ , and  $f'(z) = 0$  when  $w'(z) = 0$ . Thus saddle point locations are as usually stated. Also, as needed in (B-6),

$$\frac{f'(z)}{f(z)} = w'(z) , \quad (B-17)$$

and then (B-6) agrees with (9). Furthermore, since

$$f''(z) = [w''(z) + w'^2(z)] \exp(w(z)) ,$$

$$f''(z_s) = w''(z_s) \exp(w(z_s)) , \quad (B-18)$$

then (B-12) yields

$$\alpha = \arg w''(z_s) . \quad (B-19)$$

When (B-19) is used in (B-11), the steepest descent directions corroborate reference 1, (7.1.8) and (7.1.19). Finally, (B-16) yields

$$\arg f(z) = \arg \{\exp(w(z))\} = \arg \{\exp(u + iv)\} = v , \quad (B-20)$$

meaning that  $v$  is constant on steepest descent contours; this agrees with reference 1, Lemma 7.1.

What this all demonstrates is that, for a general given integrand  $f(z)$ , we can let  $w(z) = \ln f(z)$  and apply our usual techniques on  $w(z)$ . This procedure was adopted in the Gaussian exponent example in the main text of this report.

### References

1. N. Bleistein and R. A. Handelsman, *Asymptotic Expansions of Integrals*, Holt, Rinehart, and Winston, NY, 1975.
2. G. F. Carrier, M. Krook, and C. E. Pearson, *Functions of a Complex Variable*, McGraw-Hill Book Co., NY, 1966.
3. C. M. Bender and S. A. Orszag, *Advanced Mathematical Methods for Scientists and Engineers*, McGraw-Hill Book Co., NY, 1978.
4. Personal communication with N. Bleistein, 21 January 1981.
5. A. D. Spaulding and D. Middleton, "Optimum Reception in an Impulsive Interference Environment - Part I: Coherent Detection," *IEEE Trans. on Communications*, vol. COM-25, no. 9, September 1977, pp. 910-923.
6. F. W. J. Olver, *Asymptotics and Special Functions*, Academic Press, NY, 1974.

## INITIAL DISTRIBUTION LIST

Addressee	No. of Copies
ASN (RE&S) (D. E. Mann)	1
OUSDRE (Research & Advanced Technology (W. J. Perry))	2
Deputy USDR&E (Res & Adv Tech) (R. M. Davis)	1
OASN (Dr. R. Hoglund)	1
ONR, ONR-100, -200, -102, -222, -436	5
CNO, OP-098, -96	2
CNM, MAT-08T, -08T2, SP-20	3
DIA, DT-2C	1
NAV SURFACE WEAPONS CENTER, WHITE OAK LABORATORY	1
NRL	1
NRL, USRD	1
NORDA (Dr. R. Goodman, 110)	1
USOC, Code 241, 240	2
SUBASE LANT	1
NAVSUBSUPACNLON	1
OCEANAV	1
NAVOCEANO, Code 02	1
NAVELECSYSCOM, ELEX 03	1
NAVSEASYSCOM, SEA-003	1
NAVAL SEA SYSTEM DETACHMENT, Norfolk	1
NASC, AIR-610	1
NAVAIRDEVVCEN	1
NOSC	1
NOSC, Code 6565 (Library)	1
NAVWPNSCEN	1
DTNSRDC	1
NAVCOASTSYSLAB	1
CIVENGRLAB	1
NAVSURFWPNCEN	1
NEWES, San Diego	1
NEWES, Hawaii	1
NISC	1
NAVSUBSCOL	1
NAVPGSCOL	1
NAVWARCOL	1
NETC	1
NAVTRAEEQIPCENT (Technical Library)	1
APL/UW, Seattle	1
ARL/PENN STATE, State College	1
CENTER FOR NAVAL ANALYSES (ACQUISITION UNIT)	1
DTIC	12
DARPA	1
NOAA/ERL	1
NATIONAL RESEARCH COUNCIL	1
WEAPON SYSTEM EVALUATION GROUP	1
WOODS HOLE OCEANOGRAPHIC INSTITUTION	1
ARL, UNIV OF TEXAS	1

TR 6433

INITIAL DISTRIBUTION LIST (Cont'd)

Addressee	No. of Copies
MARINE PHYSICAL LAB, SCRIPPS	1
Dr. David Middleton, 127 East 91st St., New York, NY 10028	1
Herbert Gish, Bolt, Beranek, and Newman, 50 Moulton St., Cambridge, MA 02138	1
Prof. Louis Scharf, Dept. of Electrical Engin., Colorado State University, Fort Collins, CO 80523	1
Prof. Donald Tufts, Dept. of Electrical Engin., University of Rhode Island, Kingston, RI 02881	1
C. Hindman, TRW, Defense & Space Systems Group, One Space Park, Redondo Beach, CA 90278	1
Dr. S. L. Marple, Wash. Systems Engin. Div., The Analytic Sciences Corp., McLean, VA 22102	1
T. E. Barnard, Chesapeake Instrument Div., Gould Inc., Glen Burnie, MD 21061	1
Prof. P. M. Schultheiss, Dept. of Electrical Engin., P.O. Box 2157, Yale University, 15 Prospect Street, New Haven, CT 06520	1
Prof. Y. T. Chan, Dept. of Electrical Engin., Royal Military College, Kingston, Ontario, Canada K7L 2W3	1

**DAT**  
**FILM**